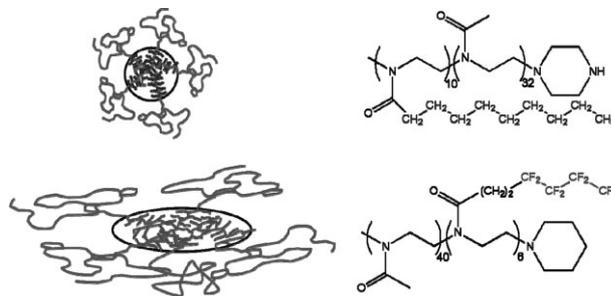# Micellar Structures of Hydrophilic/Lipophilic and Hydrophilic/Fluorophilic Poly(2-oxazoline) Diblock Copolymers in Water[a]

Ruzha Ivanova, Thomas Komenda, Tune B. Bonné, Karin Lüdtke,
Kell Mortensen, P. Klaus Pranzas, Rainer Jordan,* Christine M. Papadakis*

Amphiphilic poly(2-alkyl-2-oxazoline) diblock copolymers of 2-methyl-2-oxazoline (MOx) building the hydrophilic block and either 2-nonyl-2-oxazoline (NOx) for the hydrophobic or 2-(1H,1H′,2H,2H′-perfluorohexyl)-2-oxazoline (FOx) for the fluorophilic block were synthesized by sequential living cationic polymerization. The polymer amphiphiles form core/shell micelles in aqueous solution as evidenced using small-angle neutron scattering (SANS). Whereas the diblock copolymer micelles with a hydrophobic NOx_n block are spherical, the micelles with the fluorophilic FOx_n are slightly elongated, as observed by SANS and TEM. In water, the micelles with fluorophilic and lipophilic cores do not mix, but coexist.

R. Ivanova, T. B. Bonné, C. M. Papadakis,
Physik Department E13, Technische Universität München,
James-Franck-Str. 1, 85747 Garching, Germany
E-mail: christine.papadakis@ph.tum.de
T. Komenda, , R. Jordan, K. Lüdtke
Wacker-Lehrstuhl für Makromolekulare Chemie, Department
Chemie, Technische Universität München, Lichtenbergstr. 4,
85747 Garching, Germany
E-mail: rainer.jordan@ch.tum.de
K. Mortensen
Danish Polymer Centre, Risø National Laboratory, P.O. Box 49,
4000 Roskilde, Denmark
P. K. Pranzas
Institut für Werkstofforschung, GKSS-Forschungszentrum
Geesthacht, 21502 Geesthacht, Germany

Introduction

Amphiphilic block copolymers in aqueous solution associate reversibly into micelles, similar to low molar mass amphiphiles (for an overview see ref.[1–9]). Compared to surfactant micelles, polymer micelles are more stable and offer a much larger variety of aggregate sizes and shapes by altering the polymer architecture, composition, or structure. Functionalized polymer micelles find many applications, for example, in micellar catalysis.[10–12] Special attention is currently focused on amphiphilic polymers with fluorophilic blocks and especially ABC "multiphilic" terblock copolymers containing lipophilic, hydrophilic, and fluorophilic moieties that have been found to form multicompartment micelles in aqueous solution and, at higher concentrations, micellar networks.[13–16]

Poly(2-oxazoline)s constitute a very versatile system to study the aggregation behavior as a function of the polymer architecture and the hydrophilic/lipophilic balance. Since

WILEY
InterScience®
DISCOVER SOMETHING GREAT

Micellar Structures of Hydrophilic/Lipophilic and Hydrophilic/Fluorophilic Poly(2-oxazoline). . .

Macromolecular
Chemistry and Physics

various polymerizable 2-oxazolines are synthetically accessible and the nature of the substitution at the 2-position of the 2-oxazoline monomer unit determines the solubility of the respective polymer segment,[17] a broad variety of tailored block copolymers with diverse architectures can be synthesized. For instance, a short methyl or ethyl group in the 2-position results in a hydrophilic, whereas longer *n*-alkyl moieties such as the 2-nonyl side chain result in a hydrophobic segment. Moreover, the cationic living polymerization guarantees a good control of the block lengths at narrow molar mass distributions, and the random or gradient copolymerization of various 2-substituted 2-oxazolines is possible. Besides di- and triblock copolymers, functionalized,[11] end-capped,[14] ionic,[18] lipopolymers,[19] tetrablock,[20] as well as random or gradient[21–23] hydrophilic/hydrophobic copolymers have been synthesized.

Whereas the polymerization of 2-oxazoline monomers into hydrophilic or hydrophobic polymers and their combination into defined copolymers are widely known and their synthesis is straightforward,[24–26] reports on 2-oxazolines with perfluorinated 2-alkyl substitutions are rare because of their low reactivity in ionic polymerization, the non-trivial monomer synthesis, and the difficulties to analyze the normally insoluble polymer products. In early accounts, Saegusa et al.[27] reported on the polymerization of 2-perfluoro(*n*-alkyl)-2-oxazolines initiated by sulfonates, using the large reactivity difference between 2-*n*-alkyl and 2-perfluoro(*n*-alkyl)-2-oxazolines to develop a one-shot process for producing amphiphilic block copolymers containing pure fluorophilic segments. They also performed first studies on the surface activity of the amphiphilic diblock copolymers. Later on, Sogah and coworkers[28] synthesized amphiphilic poly(2-oxazoline) block copolymers containing fluorophilic segments with longer perfluoro(*n*-alkyl) side chains and investigated their monolayers at the air/water interface on a Langmuir-Blodgett trough as well as the adhesion of platelets on polyurethanes coated by these amphiphiles. Weberskirch and Nuyken[29] described the synthesis of water-soluble block copolymers with an end-tagged naphthalene probe containing 2-perfluoroethyl-2-oxazoline monomer units. Finally, Steinhauser and Mülhaupt[30] showed the preparation, cure behavior, and properties of bis(2-oxazoline)s containing oligo(tetrafluoroethylene) segments which form various gels. Following our preliminary account on the first defined synthesis of di and triblock copolymers consisting of 2-(1H,1H',2H,2H'-perfluorohexyl)-2-oxazoline (FOx), 2-methyl-2-oxazoline (MOx), and 2-nonyl-2-oxazoline (NOx),[31,32] we report here in more detail the monomer synthesis of FOx, its reactivity, and the preparation of block copolymers. Especially triblock copolymers with lipophilic, hydrophilic, and fluorophilic blocks[31] are promising candidates for the formation of multicompartment polymer micelles and hydrogels.

Using fluorescence correlation spectroscopy (FCS) and photon correlation spectroscopy (PCS), we have previously studied the transition from unimers (i.e., single dissolved block copolymer molecules) to micelles in aqueous solutions of diblock, triblock, and gradient copolymers from MOx and NOx.[26,33,34] After dissolving polyMOx-*block*-polyNOx) (PMOx-*b*-PNOx) diblock copolymers in water at room temperature, large metastable aggregates are present, which vanish upon prolonged heat treatment of the solutions and equilibrium is achieved.[26] The equilibrium micelles have hydrodynamic radii of the order of 10 nm. The critical micelle concentration (CMC) is typically very low ($\approx 10^{-5}$ M) and can only be detected using FCS. Using small-angle neutron scattering (SANS), we have shown that the equilibrium micelles formed by PMOx-*b*-PNOx diblock copolymers are spherical and of core/shell type.[35]

This paper presents the detailed micellar structure of a lipophilic/hydrophilic diblock copolymer, PNOx$_{10}$-*b*-PMOx$_{32}$, discussed in comparison to that of a hydrophilic/fluorophilic diblock copolymer, PMOx$_{40}$-*b*-PFOx$_6$. The copolymers of comparable block lengths differ only in the chemical nature of the hydrophobic block, thus allowing us to study its influence on the micellar structure.

Experimental Part

Materials

All solvents and reagents for the polymerization reactions were dried and distilled before use under nitrogen: acetonitrile, chloroform, chlorobenzene, 2-methyl-2-oxazoline, and 2-nonyl-2-oxazoline (distilled from CaH$_2$). All chemicals were purchased from Aldrich (München, Germany), except ethyl heptafluorobutyrate and 1H,1H,2H,2H-perfluorohexyl iodide which were obtained from ABCR (Karlsruhe, Germany), and 2-nonyl-2-oxazoline which was received as a gift from Henkel (Düsseldorf, Germany). The initiator salt, *N*-methyl-2-methyl-2-oxazolinium triflate, was synthesized from methyl triflate and 2-methyl-2-oxazoline as reported previously.[21]

Monomer Synthesis

N-(2-Hydroxyethyl)-2-perfluoropropane Acidamide (**1**)

1 was prepared by dissolving 9.77 g (0.16 mol) amino ethanol in 120 mL dry THF and adding dropwise 25.09 g (0.11 mol) ethyl heptafluorobutyrate, in 30 mL THF. The reaction mixture was stirred at room temperature for 16 h and the raw product was distilled under reduced pressure (81 °C/30 Pa). **1** was obtained in 97% yield.

^{1}H NMR (DMSO-d_6): $\delta = 9.10$ (1H, NH), 4.55 (s, 1H, OH), 3.31 (t, 2H, C*H*$_2$−OH), 3.06 (t, 2H, C*H*$_2$−NH).

^{13}C NMR (DMSO-d_6): $\delta = 157.02$ (C=O), 116.87 (CF$_3$), 108.45 (*C*F$_2$−CO), 108.06 (*C*F$_2$−CF$_3$), 58.99 (*C*H$_2$−NH), 42.55 (*C*H$_2$−OH).

^{19}F NMR (DMSO-d_6): $\delta = -81.65$ (3F, CF$_2$−CF_3), −121.50 (2F, CF_2−CO), −127.83 (2F, CF_2−CF$_3$).

N-(2-Chloroethyl)-2-perfluoropropane Acidamide (1b)

1b was prepared by refluxing 28.03 g (0.109 mol) **1** in 136 mL (1.744 mol) thionyl chloride for 16 h. After distillation, **1b** was obtained in 86% yield (62 °C/30 Pa).

^{1}H NMR (DMSO-d_6): $\delta = 9.10$ (1H, NH), 3.31 (t, 2H, CH_2−Cl), 3.06 (t, 2H, CH_2−NH).

^{13}C NMR (DMSO-d_6): $\delta = 157.02$ (C=O), 116.87 (CF$_3$), 108.45 (CF_2−CO), 108.06 (CF_2−CF$_3$), 58.99 (CH$_2$−NH), 42.55 (CH$_2$−Cl).

^{19}F NMR (DMSO-d_6): $\delta = -81.65$ (3F, CF$_2$−CF_3), −121.50 (2F, CF_2−CO), −127.83 (2F, CF_2−CF$_3$).

2-Perfluoropropyl-2-oxazoline (1c)

1c was prepared by dehydrochlorination of **1b**. A solution of 23.50 g (0.085 mol) **1b** in 100 mL THF was added dropwise to a stirred aqueous 25% KOH solution. After stirring the reaction mixture for 16 h at room temperature, and the THF was removed. The liquid residue was extracted three times with methylene dichloride. After drying over Na$_2$SO$_4$, filtration, and removal of the solvent, **1c** was isolated by distillation. Yield 12.64 g (54%); b.p. 135 °C.

^{1}H NMR (DMSO-d_6): $\delta = 4.71$ (t, 2H, CH_2−O), 4.25 (t, 2H, CH_2−N).

^{13}C NMR (DMSO-d_6): $\delta = 156.34$ (C), 119.73 (CF$_3$), 112.52 (CF_2−CF$_3$), 106.09 (CF_2−C), 69.97 (CH$_2$−O), 55.09 (CH$_2$−N).

^{19}F NMR (DMSO-d_6): $\delta = -81.65$ (3F, CF$_2$−CF_3), −117.65 (2F, CF_2−CON), −127.89 (2F, CF_2−CF$_3$).

1H,1H,2H,2H-Perfluorohexylnitrile (2a)

2a was prepared by dissolving 3.93 g (8.02 · 10^{-2} mol) NaCN in 130 mL DMSO at 85 °C. Then, 25 g (6.68 · 10^{-2} mol) 1H,1H,2H,2H-perfluorohexyl iodide was added dropwise. The reaction solution was stirred for 24 h at 85 °C. The mixture was cooled to room temperature and added to an aqueous ice/potassium carbonate mixture. The product was extracted three times with diethyl ether, the organic phases were combined and dried with MgSO$_4$. After filtration, the ether was removed under reduced pressure and 9.28 g (51%) 1H,1H,2H,2H-perfluorohexylnitrile was obtained.

^{1}H NMR (CDCl$_3$): $\delta = 2.75$−2.21 (m, 4H).

^{13}C NMR (CDCl$_3$): $\delta = 120.46$−109.21 (m, C_4F$_9$), 116.65 (CN), 55.32 (CF$_2$−CH$_2$), 41.16 (CH$_2$−CN).

^{19}F NMR (CDCl$_3$): $\delta = -81.74$ (3F, CF$_2$−CF_3), −116.10 (2F, CF_2−CH$_2$), −125.02 (2F, CF_2−CF$_2$−CH$_2$), −126.59 (2F, CF$_3$−CF_2).

2-(1H,1H′,2H,2H′-Perfluorohexyl)-2-oxazoline (FOx)[36]

2-(1H,1H′,2H,2H′-Perfluorohexyl)-2-oxazoline was prepared by dissolving 3.56 g (3.296 × 10^{-2} mol) 1H,1H,2H,2H-perfluorohexylnitrile and 0.222 g (8.24 × 10^{-4} mol) of [Cd(OAc)$_2$ · 2H$_2$O] in 33 mL dry 1-butanol and heated to 125 °C. Afterwards, 2.42 g (3.96 × 10^{-2} mol) aminoethanol was added dropwise. The mixture was stirred for 48 h at 125 °C. The product was purified via column adsorption chromatography (aluminum oxide, neutral, activity grade III, pore size 0.05–0.15 mm, ethyl acetate/hexane/triethylamine 10:5:1), and the raw product was distilled under reduced pressure. 4.01 g (44%) 2(1H,1H′,2H,2H′-perfluorohexyl)-2-oxazoline was obtained.

^{1}H NMR (CDCl$_3$): $\delta = 4.20$ (t, 2H, CH$_2$−O), 3.75 (t, 2H, CH$_2$−N), 2.55−2.35 (m, 4H).

^{13}C NMR (CDCl$_3$) $\delta = 166.35$ (C), 123.40−107.19 (m, C_4F$_9$), 67.99 (CH$_2$−O), 62.54 (CH$_2$−CF$_2$), 54.57 (CH$_2$−N), 35.23 (CH$_2$−C).

^{19}F NMR (CDCl$_3$): $\delta = -82.16$ (3F, CF$_2$−CF_3), −116.21 (2F, CF_2−CH$_2$), −125.41 (2F, CF_2−CF$_2$−CH$_2$), −126.96 (2F, CF$_3$−CF_2).

Polymerization

The synthesis of the PNOx$_{10}$-b-PMOx$_{32}$ diblock copolymer was performed as previously described using methyl triflate as an initiator and a three-fold excess of dry piperidine was used for termination (relative to the initiator amount).[26]

PMOx$_{40}$-b-PFOx$_6$ was prepared in the same manner using an acetonitrile/chlorobenzene mixture (2:1) as the solvent.[31,32]

^{19}F NMR (CDCl$_3$): $\delta = -81.68$ (3F, CF$_2$−CF_3), −115.29 (2F, CF_2−CH$_2$), −125.06 (2F, CF_2−CF$_2$−CH$_2$), −126.66 (2F, CF$_3$−CF_2).

More details can be found as Supporting Information.

Polymer Characterization

^{1}H, ^{13}C, and ^{19}F NMR spectra were recorded on an ARX 300 spectrometer (Bruker) operating at 300.13 MHz for ^{1}H, 75.45 MHz for ^{13}C, and 282.5 MHz for [19]F. Gel permeation chromatography (GPC) was performed with chloroform as the mobile phase on a Waters Liquid Chromatograph with refractive index detector. The molecular weight distributions were based on polystyrene standards (columns: Waters Ultrastyragel; pore size 10^3, 10^4, 10^5 Å). GPC with light-scattering detection was carried out using Waters Styragel HR 4E column, a waters 2414 differential refractometer, a Waters 484 UV-Detector, and a Wyatt mini-dawn light scattering detector ($\lambda = 690$ nm).

Small-Angle Neutron Scattering (SANS)

Experiments were carried out at SANS-2 at the GKSS Forschungszentrum, Geesthacht, and at SANS II at Paul-Scherrer-Institut (PSI), Switzerland. At GKSS, a wavelength, λ, of 0.58 nm ($\Delta\lambda/\lambda = 10$%) and sample-to-detector distances (SDD) of 1, 3, 9, and 21.7 m were chosen, giving an overall range of scattering vectors, q, of 0.16–2.6 nm^{-1}. The samples were mounted in standard Hellma quartz cuvettes (light path of 1 mm), and measurements were performed at room temperature (measuring times between 30 and 120 min per image). The background, measured with the solvent (D$_2$O), was subtracted from the sample scattering taking the transmissions into account. The intensities were corrected for the detector response using the scattering of polyethylene and brought to an absolute scale using the scattering of single-crystalline vanadium. All these operations were performed using the software SANDRA.[37] At PSI, the following three geometries were chosen: $\lambda = 0.45$ nm and SDD = 1 m; $\lambda = 0.45$ nm and SDD = 4 m; and $\lambda = 1.06$ nm and SDD = 6 m, resulting in an overall q-range of 0.032–3.85 nm^{-1}. Standard Hellma quartz cuvettes (light path of 1 mm) were used. The measurements were performed at room temperature for 1 h (at SDD = 1 and 6 m) and for 2 h (at SDD = 4 m). The sample scattering patterns were corrected by subtracting the background scattering measured with each D$_2$O/H$_2$O mixture (see below) and the detector electronic noise measured using boron. At this, the sample, the background, and the boron transmissions were taken into account. The images were azimuthally averaged,

Micellar Structures of Hydrophilic/Lipophilic and Hydrophilic/Fluorophilic Poly(2-oxazoline)...

Macromolecular
Chemistry and Physics

and the resulting intensities were brought to an absolute scale using the scattering of H_2O.

The scattering length densities (δ) of the polymer blocks ($\delta_{MOx} = 1.2 \times 10^{10}$ cm^{-2}; $\delta_{NOx} = 0.26 \times 10^{10}$ cm^{-2}; and $\delta_{FOx} = 3.0 \times 10^{10}$ cm^{-2}) were calculated based on the scattering length densities of the elements and the mass densities. The latter were calculated using the group contributions for the amorphous polymers:[38] 1.06 g · cm^{-3} for MOx$_n$, 0.93 g · cm^{-3} for NOx$_n$, and 1.94 g · cm^{-3} for FOx$_n$. Contrast matching of the core or the shell block was performed by using mixtures of D_2O ($\delta_{D2O} = 6.4 \times 10^{10}$ cm^{-2}) and H_2O ($\delta_{H2O} = -0.56 \times 10^{10}$ cm^{-2}) as a solvent. In all solutions, the polymer concentrations were far above the CMC, i.e., only a small fraction of the copolymers was present as unimers.[26] SANS measurements on the solution of PNOx$_{10}$-b-PMOx$_{32}$ in D_2O were performed before and after annealing at 60 °C for 24 h. The other solutions were annealed at 60 °C for 12 h prior to measurements. A mixed solution of PNOx$_{10}$-b-PMOx$_{32}$ and PMOx$_{40}$-b-PFOx$_6$ was prepared in the molar ratio 1:2, resulting in a solution with a total polymer concentration of 13.4×10^{-3} M. The solution was annealed once more at 60 °C for 12 h prior to measurement.

Analysis of the Scattering Curves

The azimuthally averaged scattering curves were analyzed using the generalized inverse Fourier transformation (GIFT) module of the PCG software.[39–41] In general, the scattering intensity as a function of the scattering vector, $I(q)$, is given by $I(q) \sim ZP(q)S(q)$, where Z is the number of the scattering objects, $P(q)$ the form factor, and $S(q)$ the structure factor. The size and the shape of the scattering objects are described by the form factor, which is related to the pair distance distribution function (PDDF). In a first step, the PDDF, $p(r)$, was calculated by inverse Fourier transformation of the scattering curves into real space without any assumption for the shape of the scattering object. The PDDF describes the probability with which a given distance within the scattering object appears. Its shape is very sensitive to the shape of the scattering object.[39,40] For instance, spherical scattering objects result in a symmetric, bell-shaped PDDF with the diameter equal to the distance at which the PDDF reaches zero.[39] For homogeneous cylindrical particles, the PDDF rises steeply as a function of radius, then decreases, first steeply, then more shallow, until it reaches zero. The cylinder radius and the length, L, are determined from the point of inflection in the decreasing part and from the radius where the PDDF reaches zero, respectively.[42] In a second step, the experimental scattering intensity is fitted using the above equation with the interparticle correlations accounted for by the structure factor,[42] which was modeled by the Percus-Yevick approximation for the interaction between micelles.[43] In this way, the micellar radius, R_M, or the core radius, R_C, depending on the scattering contrast, and the corresponding hard-sphere radius, R_{HS}, are obtained.

Transmission Electron microscopy (TEM)

The TEM micrographs were taken using a JEOL JEM2011 operated at 120 kV. Samples were prepared by placing a droplet (5 μL) of 1 wt.-% aqueous solution of PMOx$_{40}$-b-PFOx$_6$ on a holey carbon film (QUANTIFOIL, Jena, Germany) supported by a copper grid. The excess solution was blot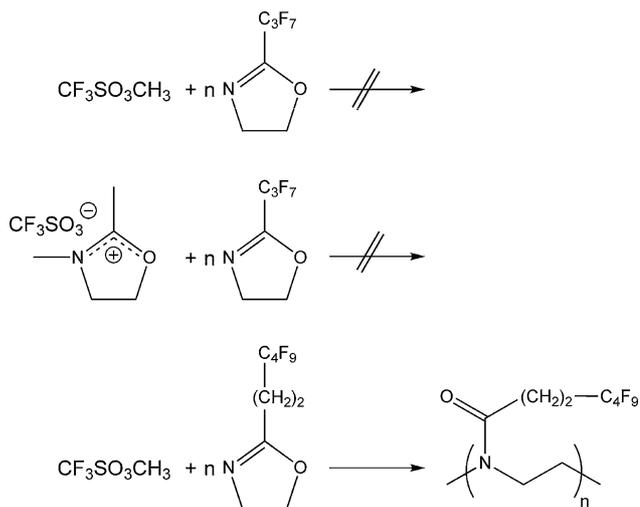ted with a filter paper. The resulting thin liquid film (thickness ≈50 nm) in the holes of the carbon film was then air-dried at room temperature.

Results and Discussion

Polymer Synthesis

The introduction of strong electron-withdrawing perfluoroalkyl substituents in the 2-position of the oxazoline ring decreases the reactivity of the monomer and of the respective propagating chain ends. Following the literature,[27] we tried to copolymerize 2-perfluoropropyl-2-oxazoline with different 2-alkyl-2-oxazoline monomers, with methyl triflate (MeOTf) as the initiator. However, nowhere, a living ionic polymerization was observed. In reactivity tests monitored in situ by ^{1}H NMR spectroscopy, using MeOTf or N-methyl-2-(methyl)-2-oxazolinium trifluoromethanesulfonate as initiators, no reaction between 2-perfluoropropyl-2-oxazoline and the initiators could be observed within 16 h at 60 °C (Scheme 1). After the addition of MeOx, both polymerization mixtures gave readily the expected poly(2-methyl-2-oxazoline) homopolymer in quantitative yields, and in the final spectra the monomer signals of 2-perfluoropropyl-2-oxazoline remained unchanged in position and intensity. Thus, it is concluded that the reactivity of 2-perfluoroalkyl-2-oxazolines is so low that under the used conditions no polymerization occurs.

At elevated temperatures (120 °C) and polymerization in bulk, minor conversion of 2-perfluoropropyl-2-oxazoline was observed and an insoluble material was formed in very low yields. Since the strong electron withdrawing perfluorinated side chain reduces the nucleophilicity of the 2-oxazoline monomer, an electronic decoupling of the

Scheme 1. Reactivity studies of perfluorinated 2-oxazoline monomers.

perfluorinated chain and the 2-oxazoline ring should yield a polymerizable monomer. This was achieved by the insertion of a short ethylene spacer in the synthesized FOx monomer. Moreover, this monomer is synthetically readily accessible via the classic Witte-Seeliger 2-oxazoline synthesis route from the corresponding nitrile.[36] In our polymerization studies, we observed the conversion of FOx via the living cationic polymerization mechanism. For instance, with MeOTf, FOx could be quantitatively converted to the corresponding homopolymer (PFOx$_n$). The GPC analysis of the fluorinated homopolymer gave a monomodal distribution and a low polydispersity index; PDI $= 1.25$. End group analysis based on the ^{1}H NMR spectroscopy data also revealed a good control of the degree of polymerization via the initial monomer to initiator ratio ([M]$_0$/[I]$_0 = 10$, DP $= 10$). In the ^{19}F NMR spectrum of PFOx$_{10}$, all four signals corresponding to the 1H,1H′,2H,2H′-perfluorohexyl side chain could be unambiguously assigned (data not shown). The FOx monomer was also successfully copolymerized under standard polymerization conditions used for the preparation of lipophilic/hydrophilic block copolymers.

The structures of the amphiphilic block copolymers PMOx$_{40}$-b-PFOx$_6$ and PNOx$_{10}$-b-PMOx$_{32}$ are outlined in Figure 1, the corresponding analytical values are compiled in Table 1.

Structural Analysis

Non-Equilibrium Aggregates

Our previous FCS and PCS experiments have shown that the PNOx$_{10}$-b-PMOx$_{32}$ diblock copolymers form large aggregates (hydrodynamic radius $r_H = 140 \pm 20$ nm) upon dissolution at room temperature in water ($c = 9 \times 10^{-3}$ M) that coexist with micelles ($r_H^{mic} = 13 \pm 2$ nm) and unimers ($r_H^{uni} = 1.2 \pm 0.5$ nm).[26] Equilibrium can be achieved by annealing the solution at 60 °C or higher, which results in solutions containing only equilibrium micelles and unimers, having the same hydrodynamic radii as before: $r_H^{mic} = 11.3 \pm 0.9$ nm and $r_H^{uni} = 1.3 \pm 0.2$ nm.[26] Here, it is
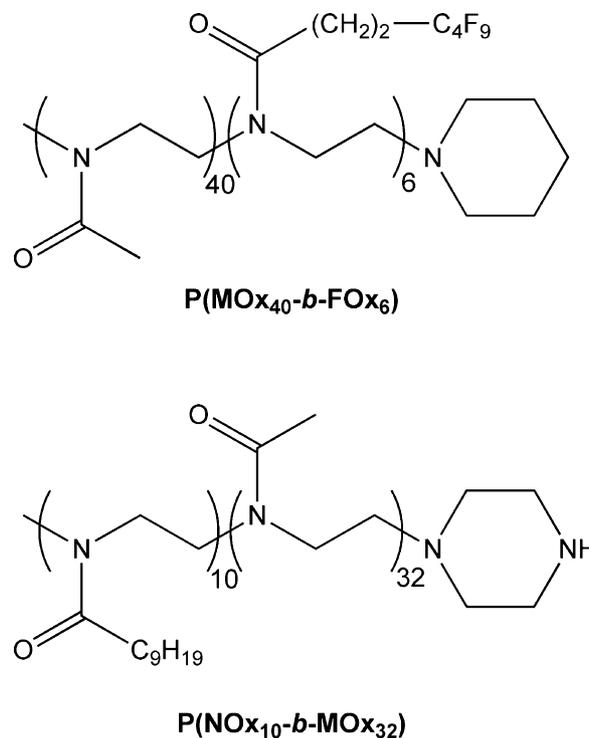

P(MOx$_{40}$-b-FOx$_6$)

P(NOx$_{10}$-b-MOx$_{32}$)

Figure 1. Structures of the synthesized copolymers PMOx$_{40}$-b-PFOx$_6$ and PNOx$_{10}$-b-PMOx$_{32}$ used for this study.

of interest to discuss the structure of the aggregates and the possible reasons of their formation.

To gain more information about the size of the aggregates, we have carried out SANS experiments on 12×10^{-3} M PNOx$_{10}$-b-PMOx$_{32}$ in D$_2$O, a concentration far above the CMC. D$_2$O was chosen to maximize the contrast between the aggregates/micelles and the solvent. The scattering curves before and after annealing at 60 °C for 24 h differ considerably (Figure 2a): Annealing leads to a significant reduction of the forward scattering. The corresponding PDDF, $p(r)$, shows two peaks prior to annealing (Figure 2b). The narrow signal located at 7.5 nm is attributed to the equilibrium micelles. The additional broad peak centered around 24 nm and finite up to ≈50 nm is attributed to the aggregates. Their size

Table 1. Analytical values of the diblock copolymers.

Polymer	[M]$_0$/[I]$_0$	[M]$_0$/[I]$_0$	DP	DP	$\overline{M}_n$ c)	Yield	PDI d)	CMC
						%		10^{-5} mol · L^{-1}
PNOx$_{10}$-b-PMOx$_{32}$	7	30	10	32	4 800	92	1.07	2.2 e)
PMOx$_{40}$-b-PFOx$_6$	30	6	40	6	5 403	78	1.26	6.47 f)

a)Initial monomer to initiator feed; b)Degree of polymerization calculated by end group analysis from ^{1}H NMR data; c)Number-average molar mass calculated from end group analysis; d)Polydispersity index: $\overline{M}_w/\overline{M}_n$ as measured by GPC; e)CMC as determined by FCS;[34a] f)As determined by fluorescence spectroscopy using free TNS as a probe.
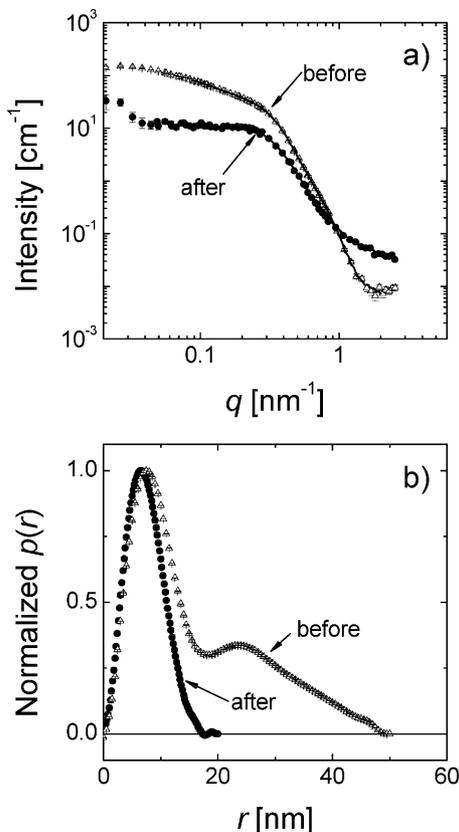
Micellar Structures of Hydrophilic/Lipophilic and Hydrophilic/Fluorophilic Poly(2-oxazoline)...

Macromolecular
Chemistry and Physics

Figure 2. (a) SANS intensity curves from solutions of PNOx$_{10}$-b-PMOx$_{32}$ in D$_2$O. Polymer concentration 5.7 wt.-% (12×10^{-3} M calculated using $\overline{M}_n$). ($\triangle$) Before and ($\bullet$) after annealing. The lines are fits determined by GIFT. (b) The corresponding PDDFs, normalized to the height of the first peak.

distribution is thus quite broad. After annealing, this broad peak vanishes, i.e., the aggregates dissolve. In contrast, the peak assigned to the micelles remains nearly unchanged in position (6.6 nm) and width. We note that the maximum position does not strictly correspond to the micellar radius, since the NOx$_{10}$-rich core and the hydrophilic MOx$_{32}$-rich shell contribute differently to the scattering curve due to their different scattering length densities. We conclude that the large non-equilibrium aggregates vanish upon annealing by reorganization of the polymer amphiphiles into equilibrium micelles.

The formation of large and metastable aggregates upon dissolution of amphiphilic block copolymers at room temperature may be due to the low solubility of the two polymer blocks in the solvent or to the kinetics of the dissolution of the solid state morphology of the polymer, which may be hampered by the high viscosity of the lipophilic block.[8,44,45] As discussed in ref.[26], in our case, the interaction of the NOx$_n$ blocks via nonyl-nonyl interactions may be at the origin of the slow kinetics of dissolution. In bulk poly(2-nonyl-2-oxazoline), the crystalline state persists up to $\approx$150 °C.[17,46]

Micelles with a Lipophilic Core

We have previously reported the core/shell structure of the micelles formed by the PNOx$_{10}$-b-PMOx$_{32}$ diblock copolymer in water.[35] Here, we discuss in detail the results obtained in SANS experiments with contrast matching and compare them to the micellar structure of a similar hydrophilic/fluorophilic diblock copolymer. We matched the scattering length density of the shell or the core with mixtures of D$_2$O and H$_2$O to determine the core size and shape and the thickness of the shell separately. The scattering curves of annealed PNOx$_{10}$-b-PMOx$_{32}$ solutions together with the corresponding PDDFs are shown in Figure 3. No forward scattering was observed, proving the absence of large aggregates. Closeness to the symmetric shape of the corresponding PDDFs (Figure 3b and d) indicates the spherical shape of the polymer micelles for both the core and the shell (see Experimental Part and ref.[39]). We conclude that the micelles are of core/shell type with NOx$_{10}$ forming the core and MOx$_{32}$ the shell. The fitting parameters obtained are compiled in Table 2.

The micellar core radius calculates to 2.6 nm. The fully stretched NOx$_{10}$ backbone length was estimated to 3.7 nm using a model minimizing the free energy of the NOx$_{10}$ block in vacuum.[48] This value is slightly larger than the core radius, hence the NOx$_{10}$ block is most probably in a stretched conformation within the micellar core. This is plausible because the NOx$_{10}$ block is short and has bulky side groups, a random coil conformation can thus be ruled
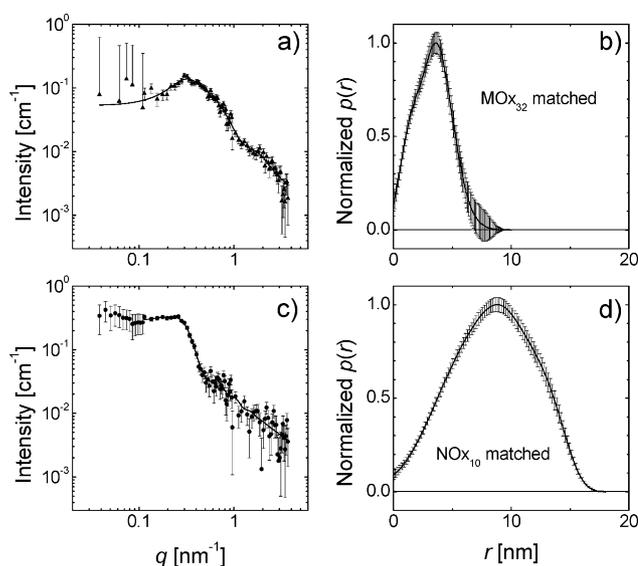

Figure 3. (a, c) SANS intensity curves from annealed solutions of PNOx$_{10}$-b-PMOx$_{32}$ in D$_2$O/H$_2$O and (b, d) corresponding PDDFs.[47] Polymer concentration 10 wt.-% (21×10^{-3} M calculated using $\overline{M}_n$). The lines in (a) and (c) are fits determined by GIFT. (a, b) MOx$_{32}$ block matched by D$_2$O/H$_2$O = 23/77 vol.-% and (c, d) NOx$_{10}$ block matched by D$_2$O/H$_2$O = 11/89 vol.-%.

Table 2. Structural parameters of the polymer micelles as derived from SANS on annealed micellar solutions.

Contrast[a]	PNOx$_{10}$-b-PMOx$_{32}$ spherical micelles		PMOx$_{40}$-b-PFOx$_6$ elongated micelles	
	Core	Shell	Core	Shell
R_C/nm	2.6		3.7	
R_M/nm		6.5		5.2
D_{shell}/nm		3.9		1.5
L/nm			13.0	15.0
R_{HS}/nm	8.1	8.9	15.1	16.3

[a]R_c: core radius, R_m: micellar radius, D_{shell}: shell thickness, L: length of the cylindrical core or micelle, R_{HS}: hard-sphere radius.

out. Another reason for the strong stretching of the NOx$_{10}$ block is the large conformational asymmetry of the diblock copolymer: The volume of the NOx monomer unit (0.35 nm^3) is approximately three times larger than the one of the MOx monomer unit (0.13 nm^3).[38] Since the areas of the two blocks at the interface of the micellar core must be equal, the more flexible and long MOx$_{32}$ block will tend to coil whereas the stiff NOx$_{10}$ block will stretch. Calculating the ratio of the core volume and the NOx$_{10}$ block volume results in an aggregation number $N_{agg} = 21$, which is relatively low but within the usual range.[6,8] N_{agg} is known to depend on the hydrophilicity of the entire polymer, the polymer concentration, and the temperature.[8] Since N_{agg} decreases with increase in hydrophilicity of the polymer, we attribute the low N_{agg} value to the fact that the NOx$_{10}$ block is relatively hydrophilic, as expected from its polysoap nature. More advanced scaling models [49,50] fail to describe the core size because of the complex chemical structure of the NOx$_{10}$ block.

The thickness of the micellar shell formed by the MOx$_{32}$ block calculates to 3.9 nm, thus significantly smaller than the fully stretched length of the MOx$_{32}$ backbone of 12.2 nm.[48] For grafted, flexible, neutral polymer chains in good solvent, the scaling concept by Alexander and de Gennes[51] describes the polymer conformation in the micellar shell. According to this model, the grafted chains are in a brush conformation if the distance between the anchoring points, D, is smaller than the radius of gyration in good solvent, R_F, which is given by $R_F = aN^{3/5}$.[52,53] Assuming a segment length not much larger than the monomer unit length, $a = 0.37$ nm,[48] which is reasonable for flexible polymers, R_F calculates to 3.0 nm. Using $D^2 = 4\pi R_C^2/N_{agg}$ for the distance between the anchoring points results in $D = 2.0$ nm, thus $D < R_F$. The thickness of

the polymer brush is then given by $L_B = aN(a/D)^{\frac{2}{3}}$ (ref.[51b]), which results in $L_B = 3.8$ nm. This value is very close to the measured shell thickness of 3.9 nm. The calculated value may be slightly overestimated because the micellar core interface is curved and not flat. Nevertheless, we conclude that the NOx$_{10}$ block is strongly stretched from the interface of the micellar core toward its center, whereas the MOx$_{32}$ block forms a polymer brush.

The experimentally determined values of the radii may be slightly underestimated for two reasons. First, the micellar shell is presumably not a hard sphere with a sharp interface toward the solvent; rather, this interface is diffuse with single polymer chains protruding far into the solvent. Theoretical studies have shown that the micellar shell profile is well described by a hyperbolic decaying density function.[4,9,49] In our approach, we may thus have underestimated the micellar radius. However, the resulting value is strongly supported by the very good agreement between the shell thickness and the polymer brush thickness. Second, a small deviation in the contrast matching is present as inferred from the shoulders of the peaks in the PDDFs (Figure 3b and d). This deviation may arise because the densities of the core and the shell in the polymer micelle may differ from the literature values of the amorphous bulk polymers which were used for contrast matching. However, both contrasts give consistent hard-sphere radii (8.1 and 8.9 nm), which are larger than the micellar radius, as expected for the correlation distance between the micelles.

As expected, the micellar radius obtained by SANS ($R_M = 6.5$ nm) is significantly smaller than the hydrodynamic radius determined previously by FCS ($R_h = 11.3 \pm 0.9$ nm).[26,34] This is reasonable because R_h in addition to R_M comprises the shell of water bound to the shell as well as single shell blocks extending into the solvent and drawing along water molecules.

Micelles with a Fluorophilic Core

We have investigated micellar solutions of the hydrophilic/fluorophilic PMOx$_{40}$-b-PFOx$_6$ diblock copolymer using SANS with contrast matching. However, exact contrast matching of the FOx$_6$ core block for qualitative determination of the core radius is not straightforward since the mass density of FOx$_n$ is not known. Moreover, the side group of FOx$_n$ includes the ethyl spacer along with the fluorinated butyl chain, i.e., a complex structure in itself. Nonetheless, we have attempted contrast matching using the group contributions for estimating the mass density.[38] The core radius and thus also the shell thickness obtained may thus be slightly biased.

From the obtained PDDFs (Figure 4), we conclude that the hydrophilic/fluorophilic PMOx$_{40}$-b-PFOx$_6$ diblock copolymer forms core/shell micelles as well. The shoulders (Figure 4b) as well as the broad maximum in the PDDFs
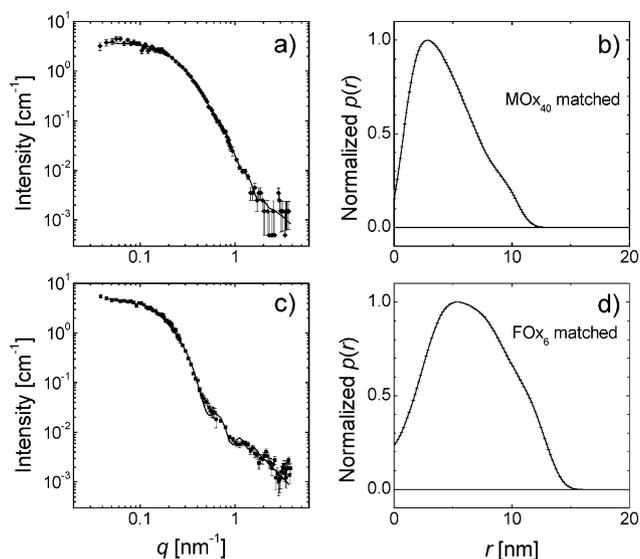
Micellar Structures of Hydrophilic/Lipophilic and Hydrophilic/Fluorophilic Poly(2-oxazoline)...

Macromolecular
Chemistry and Physics

Figure 4. (a, c) SANS intensity curves from annealed solutions of PMOx$_{40}$-*b*-PFOx$_6$ in D$_2$O/H$_2$O and (b, d) corresponding PDDFs. The lines in (a) and (c) are fits determined by GIFT. (a, b) MOx$_{40}$ block matched by D$_2$O/H$_2$O = 23/77 vol.-%, polymer concentration 6.2 wt.-% (11 × 10^{-3} M calculated using $\overline{M}_n$) and (c, d) FOx$_6$ block matched by D$_2$O/H$_2$O = 57/43 vol.-%, polymer concentration 6.3 wt.-% (12 × 10^{-3} M).

(Figure 4d) reflect the error in contrast matching. Nonetheless, the asymmetric shapes of both PDDFs indicate an elongated shape of the micelles.[39,40]

The radius and the length of the FOx$_6$ core were found to be $R_C = 3.7$ nm and $L = 13$ nm (see Table 2). The fully stretched length of one Fox monomer unit is estimated to be 0.39 nm,[48] and the fully stretched length of the FOx$_6$ block including the terminal piperidine group (0.56 nm[48]) amounts to 2.9 nm, which is smaller than R_C. We attribute this mismatch to the bias in contrast matching. The result is consistent with a stretched conformation of the FOx$_6$ block, which should be even stronger than in the NOx$_{10}$ block, because of the larger cross-section of the perfluoro-hexyl side chains; the volume of one CF$_3$ group is 0.035 nm^3 versus 0.023 nm^3 for one CH$_3$ group.[38] This leads to even higher steric and entropic demands on the backbone.

From the core volume, we estimated $N_{agg} = 266$ which is significantly higher than the one of the micelles formed by PNOx$_{10}$-*b*-PMOx$_{32}$ but still within the usual range.[8] Apart from the bias due to incomplete contrast matching, the high N_{agg} may be due to the following reasons: First, in an elongated micelle, the core blocks do not need to be stretched as much as in a spherical micelle, and thus more polymers can be accommodated. Second, because of the perfluorination, the FOx$_n$ block is more hydrophobic than the NOx$_n$ block.[8] Third, unusually large aggregation numbers have been found to originate from impurities or

from fractions of the block copolymer with a lower CMC (i.e., more hydrophobic fractions),[49] and PMOx$_{40}$-*b*-PFOx$_6$ has a higher polydispersity index than PNOx$_{10}$-*b*-PMOx$_{32}$, see Table 1.

The shell thickness was estimated to be 1.5 nm. This value is much smaller than the one obtained from the above-described polymer brush model: with $a = 0.39$ nm and $D^2 = 2\pi(2R_C^2 + R_C L)/N_{agg}$ (the core/shell interface is taken as a cylinder end-capped by two half spheres), L_B is expected at 6.9 nm. Again, the bias in contrast matching and the use of a model with a sharp interface of the shell toward the solvent may be at the origin of the mismatch.

In spite of the difficulties to reveal the details of the inner structure of the polymer micelle, the hard-sphere radii could successfully be determined at 15.1 and 16.3 nm for the two contrasts. The values do not depend on the contrast used, i.e., the description of the micellar correlations is consistent. Also for this polymer, the hard-sphere radii are larger than the determined micellar radius and length, as expected.

We conclude that PMOx$_{40}$-*b*-PFOx$_6$ forms elongated core/shell micelles in aqueous solution. Whereas the core size seems to be overestimated, the shell size is underestimated; the hard-sphere radius being revealed correctly.

The essential difference of the PMOx$_{40}$-*b*-PFOx$_6$ micelles from the ones of PNOx$_{10}$-*b*-PMOx$_{32}$ is their elongated shape. By TEM (Figure 5), the elongated shape of the micelles could be confirmed, and the diameter and length were found to be 8.8 and 14.4 nm, i.e., in good agreement with the SANS results (8.9 and 14 nm). We did not perform a cryo-TEM experiment, in spite of the higher resolution, because the electron beam would have destroyed the sample. Recently, in spin-coated thin films of tetrablock poly(2-oxazoline)s, elongated micelles were observed by TEM,[20] in contrast to earlier electron micrographs of thin films of poly(2-ethyl-2-oxazoline)-*block*-poly(2-nonyl-2-
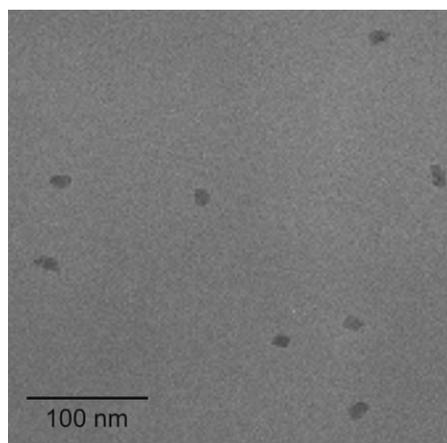

Figure 5. Electron micrograph of 1 wt.-% air-dried solution of PMOx$_{40}$-*b*-PFOx$_6$ in H$_2$O.

oxazoline) showing only spherical micelles.[54] The authors attributed the elongated shape of the micelles to the complex micelle preparation procedure and to residual solvent swelling of the micellar core, leading to non-equilibrium micelles.[20] In the present study, the polymer solutions used for TEM were prepared in the same way as for SANS measurements, i.e., by dissolution of the polymer in water, by subsequent annealing under the same conditions, and air-drying. No changes of the micellar shape have been observed for aqueous solutions of polystyrene-*block*-poly(4-vinylpyridine) during air-drying.[49] Therefore, we do not expect substantial changes of the micellar shape of $PMOx_{40}$-*b*-$PFOx_6$ either. A control TEM experiment of spherical $PNOx_{10}$-*b*-$PMOx_{32}$ micelles was not possible because the micellar core is much smaller and the core/shell electron density contrast is much lower than the one of the $PMOx_{40}$-*b*-$PFOx_6$.

Non-spherical micelles have been predicted[55] and experimentally observed with diblock copolymers containing very hydrophobic[56] or fluorinated blocks.[12,14,57] Conformational changes from spherical to disk-like shape of carbosilane dendrimers after introducing perfluoroalkyl end groups have been reported as well.[58]

We conclude that both, $PNOx_{10}$-*b*-$PMOx_{32}$ and $PMOx_{40}$-*b*-$PFOx_6$, form core/shell micelles. The core radii indicate stretching of the hydrophobic NOx_{10} and FOx_6 core blocks. The micelles formed by $PMOx_{40}$-*b*-$PFOx_6$ are elongated, which is presumably due to the stiffness and the strong repulsion of the fluorinated FOx_6 side chains from the environment.

Mixed or Coexisting Micelles?

Poly(2-oxazoline) terblock copolymers with lipophilic, hydrophilic, and fluorophilic blocks are promising candidates for the formation of multicompartment hydrogels.[59] A prerequisite is that the NOx_n and FOx_n blocks do not mix. In order to verify that these two blocks do not form common micelles, but remain in separate micellar cores, we have studied mixtures of micellar solutions of $PNOx_{10}$-*b*-$PMOx_{32}$ and $PMOx_{40}$-*b*-$PFOx_6$. If the micelles remain separate, a $PNOx_n$-*b*-$PMOx_m$-*b*-$PFOx_k$ triblock copolymer will consequently result in a multicompartment system.

The SANS scattering curve of the annealed mixed solution is shown in Figure 6. We considered several cases: (i) mixed spherical micelles, (ii) mixed elongated micelles, or (iii) separate micelles. The curves could not be modeled satisfactorily with models (i) and (ii); i.e., the parameters obtained were not meaningful, for instance, the hard-sphere radius of the core, R_{HS}, was smaller than its radius, R_C. However, good agreement was obtained (Figure 6) with a weighted addition of the scattering curves from the single components (Figure 3a and 4a) comprising spherical NOx_{10} and cylindrical FOx_6 cores.
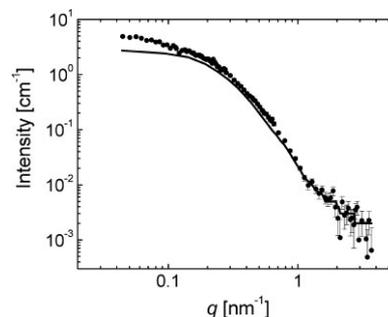

Figure 6. SANS intensity curve from an annealed mixed solution of $PNOx_{10}$-*b*-$PMOx_{32}$ and $PMOx_{40}$-*b*-$PFOx_6$ in $D_2O/H_2O = 23/77$ vol.-% (MOx_{10} block matched). Total polymer concentration 13.4×10^{-3} M. The line is the weighted sum of the fitted scattering curves from the pure $PNOx_{10}$-*b*-$PMOx_{32}$ (Figure 3a) and pure $PMOx_{40}$-*b*-$PFOx_6$ (Figure 4a).

Taking into account the strong segregation of lipophilic from fluorophilic moieties, these results indicate that the micelles with lipophilic and fluorophilic cores remain separated in aqueous environment. Similar results have been reported for other polymer systems, showing the incompatibility of hydrocarbon and fluorocarbon domains and their microphase segregation into separate domains.[13,14,15a]

Recently, Kubowicz et al.[60] reported on the morphology of micelles of telechelic poly(2-methyl-2-oxazoline)s with a short hydrocarbon chain at one end and a short perfluorinated alkyl tail on the other. In this case, the lipophilic and fluorophilic moieties mixed into micelles of cylindrical shape. Since the chemical structure and the relative size of the hydrophilic, lipophilic, and fluorophilic segments play an important role, this difference to our results nicely demonstrates that the poly(2-oxazoline) system allows the preparation of a broad variety of polymer amphiphiles such as telechelics and block copolymers that differ very much in their self-assembly behavior.

Conclusion

In contrast to literature reports, 2-perfluoropropyl-2-oxazoline, a 2-oxazoline monomer with a perfluorinated *n*-alkyl side chain in the 2-position, could not be converted to the respective homopolymers nor did a copolymerization with, e.g., 2-methyl-2-oxazoline result in a copolymer. Only after electronic decoupling of the strong electron withdrawing perfluorinated moiety from the 2-oxazoline ring, a reactive monomer [2-(1H,1H',2H,2H'-perfluoro-hexyl)-2-oxazoline; FOx] was obtained. FOx was block copolymerized with MOx to a well-defined fluorophilic/hydrophilic diblock copolymer ($PMOx_{40}$-*b*-$PFOx_6$). The structure of the micelles formed by this copolymer in

Micellar Structures of Hydrophilic/Lipophilic and Hydrophilic/Fluorophilic Poly(2-oxazoline)...

Macromolecular
Chemistry and Physics

water was compared to the one of the lipophilic/hydrophilic copolymer having a comparable hydrophilic block and a lipophilic block composed of 2-nonyl-2-oxazoline (NOx) units, $PNOx_{10}$-b-$PMOx_{32}$.

Confirming our previous FCS and PCS results, the SANS experiments showed that, upon dissolution in water at room temperature, $PNOx_{10}$-b-$PMOx_{32}$ aggregates into well-defined micelles coexisting with large metastable aggregates. These aggregates vanish upon annealing of the solution, leaving only defined equilibrium micelles. The micelles are of spherical core/shell type with a hydrophobic NOx_{10} core and a flexible hydrophilic MOx_{32} shell. The core radius and the shell thickness show that the NOx_{10} block is strongly stretched, whereas the shell formed by the MOx_{32} can be described as a polymer brush in good solvent.

In water, $PMOx_{40}$-b-$PFOx_6$ forms elongated core/shell micelles, presumably due to the higher stiffness of the perfluorinated side chains and the strong segregation of the FOx_6 block from the environment.

The micelles formed by $PMOx_{40}$-b-$PFOx_6$ and $PNOx_{10}$-b-$PMOx_{32}$ do not mix but coexist as micelles with pure lipophilic and fluorophilic cores. Currently, studies on the synthesis and aggregation behavior of triblock copolymers with lipophilic, hydrophilic, and fluorophilic segments are ongoing in our laboratories.[33,59]

[1] Z. Tuzar, P. Kratochvíl, "Micelles of Block, Graft Copolymers in Solution", in: *Surface and Colloid Science*, Vol. 15, E. Matijević, Ed., Plenum Press, New York 1993, p. 1.

[2] B. Chu, *Langmuir* **1995**, *11*, 414.

[3] N. S. Cameron, M. K. Corbierre, A. Eisenberg, *Can. J. Chem.* **1999**, *77*, 1311.

[4] I. W. Hamley, "*The Physics of Block Copolymers*", Oxford Science Publications, Oxford 1998, p. 131.

[5] S. Förster, M. Antonietti, *Adv. Mater.* **1998**, *10*, 195.

[6] P. Alexandridis, B. Lindman, "*Amphiphilic Block Copolymers: Self-assembly and Applications*", Elsevier, Amsterdam 2000.

[7] [7a] J. C. M. Van Hest, D. A. P. Delnoye, M. W. P. L. Baars, C. Elissen-Roman, M. H. P. Van Genderen, E. W. Meijer, *Chem. Eur. J.* **1996**, *2*, 1616; [7b] I. Gitsov, K. R. Lambrych, V. A. Remnant, R. Pracitto, *J. Polym. Sci., Part A: Polym. Chem.* **2000**, *38*, 2711.

[8] G. Riess, *Prog. Polym. Sci.* **2003**, *28*, 1107.

[9] E. B. Zhulina, M. Adam, I. LaRue, S. S. Sheiko, M. Rubinstein, *Macromolecules* **2005**, *38*, 5330.

[10] M. Antonietti, S. Förster, S. Oestreich, *Macromol. Symp.* **1997**, *121*, 75.

[11] P. Persigehl, R. Jordan, O. Nuyken, *Macromolecules* **2000**, *33*, 6977.

[12] T. Kotré, O. Nuyken, R. Weberskirch, *Macromol. Rapid Commun.* **2002**, *23*, 871.

[13] K. Stähler, J. Selb, F. Candeau, *Langmuir* **1999**, *15*, 7565.

[14] R. Weberskirch, J. Preuschen, H. W. Spiess, O. Nuyken, *Macromol. Chem. Phys.* **2000**, *201*, 995.

[15] [15a] A. Kotzev, A. Laschewsky, P. Adriaensens, J. Gelan, *Macromolecules* **2002**, *35*, 1091; [15b] A. Laschewsky, *Curr. Opin. Colloid Interface Sci.* **2003**, *8*, 274; [15c] J.-F. Lutz, A. Laschewsky, *Macromol. Chem. Phys.* **2005**, *206*, 813.

[16] [16a] Z. Zhou, Z. Li, Y. Ren, M. A. Hillmyer, T. P. Lodge, *J. Am. Chem. Soc.* **2003**, *125*, 10182; [16b] Z. Li, E. Kesselman, Y. Talmon, M. A. Hillmyer, T. P. Lodge, *Science* **2004**, *306*, 98; [16c] T. P. Lodge, M. A. Hillmyer, Z. Zhou, Y. Talman, *Macromolecules* **2004**, *37*, 6680.

[17] M. Litt, F. Rahl, L. G. Roldan, *J. Polym. Sci. A-2* **1969**, *7*, 463.

[18] J.-S. Park, Y. Akiyama, Y. Yamasaki, K. Kataoka, *Langmuir* **2007**, *23*, 138.

[19] [19a] R. Jordan, K. Martin, H. J. Rädler, K. Unger, *Macromolecules* **2001**, *34*, 8858; [19b] Th. R. Baekmark, T. Wiesenthal, P. Kuhn, A. Albersdörfer, O. Nuyken, R. Merkel, *Langmuir* **1999**, *15*, 3616.

[20] R. Hoogenboom, F. Wiesbrock, M. A. M. Leenen, H. M. L. Thijs, H. Huang, C.-A. Fustin, P. Guillet, J.-F. Gohy, U. S. Schubert, *Macromolecules* **2007**, *40*, 2837.

[21] R. Luxenhofer, R. Jordan, *Macromolecules* **2006**, *39*, 3509.

[22] R. Hoogenboom, M. W. Fijten, U. S. Schubert, *J. Polym. Sci., Part A: Polym. Chem.* **2004**, *42*, 1820.

[23] S. Huber, R. Jordan, *Colloid. Polym. Sci.* **2008**, *286*, 395.

[24] For reviews see e., g., [24a] K. Aoi, M. Okuda, *Prog. Polym. Sci.* **1996**, *21*, 151; [24b] S. Kobayashi, *Prog. Polym. Sci.* **1990**, *15*, 751.

[25] M. B. Foreman, J. P. Coffman, M. J. Murcia, S. Cesana, R. Jordan, C. A. Naumann, *Langmuir* **2003**, *19*, 326.

[26] T. B. Bonné, K. Lüdtke, R. Jordan, P. Štěpánek, C. M. Papadakis, *Colloid Polym. Sci.* **2004**, *282*, 833 and 1425 (Erratum).

[27] [27a] M. Miyamoto, K. Aoi, T. Saegusa, *Macromolecules* **1988**, *21*, 1880; [27b] M. Miyamoto, K. Aoi, T. Saegusa, *Macromolecules* **1989**, *22*, 3540; [27c] M. Miyamoto, K. Aoi, T. Saegusa, *Macromolecules* **1991**, *22*, 11; [27d] T. Saegusa, S. Kobayashi, K. Aoi, M. Miyamoto, *Macromol. Chem., Macromol. Symp.* **1990**, *32*, 1.

[28] [28a] J. M. Rodriguez-Parada, M. Kaku, D. Y. Sogah, *Macromolecules* **1994**, *27*, 1571; [28b] M. Kaku, L. C. Grimminger, D. Y. Sogah, S. L. Haynie, *J. Polym. Sci., Part A: Polym. Chem.* **1994**, *32*, 2187.

[29] R. Weberskirch, O. Nuyken, *J. Macromol. Sci., Part A: Pure Appl. Chem.* **1999**, *36*, 843.

[30] N. Steinhauser, R. Mülhaupt, *Macromol. Rapid Commun.* **1994**, *15*, 365.

[31] T. Komenda, R. Jordan, *Polym. Prepr.* **2003**, *44*, 986.

[32] T. Komenda, *PhD Thesis*, TU München, München **2004**.

[33] T. Komenda, K. Lüdtke, R. Jordan, R. Ivanova, T. B. Bonné, C. M. Papadakis, *Polym. Prepr.* **2006**, *47*, 197.

[34] [34a] T. B. Bonné, K. Lüdtke, R. Jordan, C. M. Papadakis, *Colloid Polym. Sci.* **2007**, *285*, 491; [34b] T. B. Bonné, K. Lüdtke, R. Jordan, C. M. Papadakis, *Macromol. Chem. Phys.* **2007**, *208*, 1402.

[35] C. M. Papadakis, R. Ivanova, K. Lüdtke, K. Mortensen, P. K. Pranzas, R. Jordan, *J. Appl. Crystallogr.* **2007**, *40*, 361.

[36] H. Witte, W. Seeliger, *Liebigs Ann. Chem.* **1974**, 996.

[37] P. Biemann, M. Haese-Seiller, P. Staron, *Physica B* **2000**, *276*, 156.

[38] D. W. van Krevelen, ''Volumetric Properties'', in: *Properties of Polymers*, Elsevier, Amsterdam 1990, Chapter 4, p. 71.

[39] O. Glatter, *J. Appl. Crystallogr.* **1977**, *10*, 415.

[40] O. Glatter, *J. Appl. Crystallogr.* **1980**, *13*, 577.

[41] A. Bergman, J. Brunner-Popela, G. Fritz, T. Früwirth, O. Glatter, J. Innerlohninger, R. Mittelbach, B. Weyerich, *PCG-Software Version 2.02.05*. Institut für Chemie, Universität Graz 1999.

[42] J. Brunner-Popela, O. Glatter, *J. Appl. Crystallogr.* **1997**, *30*, 431.

[43] J. K. Percus, G. J. Yevick, *Phys. Rev.* **1958**, *110*, 1.

[44] [44a] J. Stejskal, Č. Koňák, M. Helmstedt, P. Kratochvíl, *Collect. Czech. Chem. Commun.* **1993**, *58*, 2282; [44b] C. Price, *Pure Appl. Chem.* **1983**, *55*, 1563.

[45] P. Munk, ''Equilibrium, Nonequilibrium Micelles'', in: *Solvents and Self-Organization of Polymer*, S. E. Webber, P. Munk, Z. Tuzar, Eds., NATO, ASI Series E: Applied Sciences Vol. 327, Kluwer Academic Publisher, Dordrecht 1996, pp. 19–32.

[46] T. G. Bassiri, A. Levy, M. Litt, *J. Polym. Sci. B* **1967**, *5*, 871.

[47] These data were first communicated in ref.[35] and are displayed here for comparison and to facile discussion in the later sections.

[48] Estimated using CS Chem 3D ultra 7.0.0.

[49] S. Förster, S. Zisenis, E. Wenz, M. Antonietti, *J. Chem. Phys.* **1996**, *104*, 9956.

[50] T. Uneyama, M. Doi, *Macromolecules* **2005**, *38*, 5817.

[51] [51a] S. Alexander, *J. Phys. (Paris)* **1977**, *38*, 983; [51b] P. G. de Gennes, *Macromolecules* **1980**, *13*, 1069.

[52] P. Flory, ''Principles of Polymer Chemistry'', Cornell University Press, Ithaca, NY 1956.

[53] P. G. de Gennes, ''Scaling Concepts in Polymer Physics'', Cornell University Press, Ithaca, NY 1979.

[54] Th. R. Baekmark, I. Sprenger, M. Ruile, O. Nuyken, R. Merkel, *Langmuir* **1998**, *14*, 4222.

[55] A. N. Semenov, I. A. Nyrkova, A. R. Khokhlov, *Macromolecules* **1995**, *28*, 7491.

[56] J. Wu, E. M. Pearce, T. K. Kwei, A. A. Lefebvre, N. P. Balsara, *Macromolecules* **2002**, *35*, 1791.

[57] W. F. Edmonds, Z. Li, M. A. Hillmyer, T. P. Lodge, *Macromolecules* **2006**, *39*, 4526.

[58] K. Lorenz, H. Frey, B. Stühn, R. Mülhaupt, *Macromolecules* **1997**, *30*, 6860.

[59] R. Ivanova, T. Komenda, R. Jordan, C. M. Papadakis, in preparation.

[60] S. Kubowicz, A. F. Thünemann, R. Weberskirch, H. Möhwald, *Langmuir* **2005**, *21*, 7214.